Supporting Information for

A Simple Route to Highly Active Single-Enzyme Nanogels

Ana Beloqui,[a,b*‡] *Andrei Yu. Kobitski,*[c] *Gerd Ulrich Nienhaus,*[a,c,d,e] *Guillaume Delaittre*[a,b*]

[a]Institute of Toxicology and Genetics, Karlsruhe Institute of Technology (KIT), Hermann-von-Helmholtz-Platz 1, 76344 Eggenstein-Leopoldshafen, Germany

[b]Preparative Macromolecular Chemistry, Institute for Technical Chemistry and Polymer Chemistry, Karlsruhe Institute of Technology (KIT), Engesserstrasse 15, 76131 Karlsruhe, Germany

[c]Institute of Applied Physics, Karlsruhe Institute of Technology (KIT), Wolfgang-Gaede-Strasse 1, 76131 Karlsruhe, Germany

[d]Institute of Nanotechnology, Karlsruhe Institute of Technology (KIT), Hermann-von-Helmholtz-Platz 1, 76344 Eggenstein-Leopoldshafen, Germany

[e]Department of Physics, University of Illinois at Urbana-Champaign, Urbana, Illinois 61801, USA

[‡]Present Address: Nanomaterials group, CICnanoGUNE, Avenida Tolosa 76, 20018 Donostia-San Sebastián, Spain

a.beloqui@nanogune.eu; guillaume.delaittre@kit.edu

Index

1. Materials 4

2. Characterization methods 5-6

2.1. Protein concentration measurements 5

2.2. UV-Vis spectroscopy // Activity measurements 5-6

2.3. Dynamic Light Scattering (DLS) 6

2.4. Confocal microscopy 6

3. Synthesis of SENs 7-10

3.1. Acryloylation of enzymes 7

3.2. In situ polymerization/encapsulation 7-8

3.3. Evaluation of the effect of sucrose 8-10

4. GOx as case of study 10-15

4.1. Tuning SEN thickness 10-11

4.2. GOx_SEN chromatographic analysis 12-15

5. Extension to other proteins 15-17

5.1. Thickness vs protein concentration dependence 15-16

5.2. Stabilization of laccase TvL at physiological conditions 17

6. Enzymatic activity tests 18-24

6.1. GOx 18-21

6.1.1. Determination of the kinetic parameters at different shell thicknesses *18-20*

6.1.2. Stability of GOx_SENs *20-21*

6.1.3. Production of GOx_SENs with invariable activity over the entire pH range (GOX_SEN11) *21-22*

6.2. Other enzymes 22-25

7. Single particle analysis 25-32

7.1. Blank experiment 25-26

7.2. Calibration curves 26-27

7.3. Catalysis selection for thio-Michael addition-based hydrogel labeling 27-29

7.4. Labeling of HRP 29-30

7.5. Encapsulation of labeled HRP 30-31

7.6. Labeling of the shell of core-labeled SENs 31

7.7. Single-particle burst coincidence analysis *32*

8. References **33**

1. Materials

Acrylamide (AAm; 99.9%, Carl Roth), *N,N´*-methylenebisacrylamide (MBAAm; > 99%, Acros), ammonium persulfate (APS; 98%,), tetramethylethylenediamine (TEMED; 99%), 4-(dimethylamino)antipyrine (AP; 98%, ABCR), 2,2'-azino-bis(3-ethylbenzothiazoline-6-sulphonic acid) (ABTS; Panreac AppliChem), hydrogen peroxide (35 % v/v in water, Carl Roth), *D*-glucose (≥ 95%, Carl Roth), tris(2-carboxyethyl)phosphine (TCEP; 98%, Carl Roth), *N,N*-diisopropylethylamine (DIPEA; ≥ 99%), *N*-hydroxysuccinimide (NHS-OH; 98%, Sigma), 1-ethyl-3-(3-dimethylaminopropyl)carbodiimide hydrochloride (EDC-HCl; ≥ 98%, Sigma), Alexa Fluor 647 carboxylic acid tris(triethylammonium) salt (Alexa 647; ThermoFisher Scientific), and rhodamine-PEG-thiol (Rho-PEG-SH; MW 3400, Nanocs) were used as received without further purification. Rhodamine 6G methacrylate (RMA) was synthesized according to a previously reported procedure.[1] Glucose oxidase from *Aspergillus niger* (GOx; E.C. 1.1.3.4, 108 U/mg, Amresco), horseradish peroxidase (HRP; E.C. 1.11.1.7, > 1100 U/mg, Alfa Aesar), ß-glucosidase from almonds (β-Glu; E.C. 3.2.1.21, ≥ 6 U/mg, Sigma), lipase B from *Candida albicans* (CalB; E.C. 3.1.1.3, 0.4 U/mg, Sigma), esterase from *Pseudomonas fluorescens* (PfE; E.C. 3.1.1.1, ≥ 4 U/mg, Sigma), alcohol oxidase from *Pichia pastoris* (AOx; E.C. 1.1.3.13, 10-40 U/mg, Sigma), catalase from *Corynebacterium glutamicum* (Cat; E.C. 1.11.1.6, ≥ 500 KU mL^{-1}, Sigma), laccase from *Trametes versicolor* (TvL; E.C. 1.10.3.2, ≥ 0.5 U/mg, Sigma), and bovine serum albumin (BSA; Sigma) were kept at –20 °C until used. Unless specified, solvents were of analytical grade and were purchased from VWR or Fisher Scientific. All buffers were freshly prepared and filtered through 0.22 µm filters prior to use. Filter membranes (30 and 10 kDa MWCO, Vivaspin 6, Sartorius), dialysis membranes (10 kDa MWCO, Spectra/Por® 6,

SpectrumLabs), and Sephadex columns (Sephadex™ G-75 and PD-miditrap G-25, GE Healthcare) were used for concentration and purification of enzymes and SENs.

2. Characterization methods

2.1. Protein concentration measurement. Native protein concentrations were determined by measuring in a Biotek Epoch 2 spectrophotomer the absorbance at 280 nm using UV-transparent quartz cuvettes with a 1 cm path length. Molar extinction coefficients (in M^{-1} cm^{-1}) used for the calculation are the followings: 41285 (for CalB), 61100 (for TvL), 45000 (for ß-Glu), 246000 (for Cat), 93500 (for AOx), 14100 (for BSA), and 36600 (for PfE). Proteins and SENs containing chromogenic cofactors were measured at their specific wavelength: 402 nm and 102000 M^{-1} cm^{-1} for HRP; 450 nm and 14100 M^{-1} cm^{-1} for GOx.

Due to partial absorption by the polyacrylamide polymer at 280 nm, protein concentration of the nanogel solutions were also measured using the Bradford assay.[2]

2.2. UV-Vis spectroscopy // Activity measurements. Activity assays were performed at 40 ºC in 96-well plates with 200 µL as final volume per well. Unless specified in the text, HRP activity assays were performed upon mixing H_2O_2 (2.9 mM) and ABTS (0.27 mM) in sodium citrate buffer (50 mM, pH 5.1). *D*-glucose (2 mg mL^{-1}), ABTS (0.27 mM) and a HRP solution (0.01 mg mL^{-1}) in phosphate buffer (50 mM, pH 6.0) were used for the assessment of the catalytic activity of GOx. TvL activity was measured using ABTS (0.3 mM) as substrate in sodium acetate buffer (50 mM, pH 6.0). For these enzymes, the absorption arising from oxidized ABTS was monitored at 416 nm and a molar attenuation coefficient of 36000 M^{-1} cm^{-1} was used for the calculations.

Both CalB and PfE activity was monitored with the hydrolysis of *p*-nitrophenylbutyrate (*p*NPC$_4$, 0.8 mM) in Tris-HCl buffer (100 mM, pH 7.0). β-Glu activity assay was performed with *p*-nitrophenyl glucopyranoside (*p*-NPGluc, 1 mM) in Tris-HCl buffer (100 mM, pH 8.0). In both cases, the release of *p*-nitrophenol was recorded at 405 nm and an extinction coefficient of 13400 M^{-1} cm^{-1} was used for calculations.

2.3 Dynamic light scattering (DLS). DLS measurements were performed on a Malvern Zetasizer Nano ZS. Proteins and SENs were prepared at 1 mg mL^{-1} in 30 mM phosphate buffer and filtered through 0.22 μm membranes. Experiments were performed at 22 °C and 13 readouts were taken in three independent measurements for each sample.

2.4 Confocal microscopy. Single-particle fluorescence measurements were performed on freely diffusing molecules using a home-built confocal microscope based on a Zeiss Axiovert 135 frame.[3,4] Two-channel detection and an alternating excitation scheme were utilized as described elsewhere.[5] Briefly, solutions containing ~100 pM of HRP and nanogel nanoparticles were placed in a glass sample cell. Green (532 nm from an Excelsior 532 Nd-YAG laser, Spectra Physics, Mountain View, CA, USA) and red (637 nm from an Obis 637 OPS laser, Coherent Inc., Santa Clara, CA, USA) laser irradiation was rapidly alternated (10 kHz, 50% duty cycle) to excite fluorescently labelled nanoparticles during their brief travel (typically 1 – 2 ms) through the confocal volume. Emitted light was collected by a water-immersion objective (UPlan Apo 60×/1.2w Olympus, Hamburg, Germany), passed through a 100 μm pinhole, and registered in two spectral channels (Notch 532 filter, Semrock; 640DCXR dichroic, Chroma; Brightline HC 580/60, Semrock; HC 642/LP, Semrock; all via AHF, Tübingen, Germany) with SPAD detectors

(SPCM-AQR-14, Perkin Elmer Optoelectronics, Boston, MA, USA, and COUNT-100C, Laser Components, Olching, Germany).

3. Synthesis of SENs

3.1 Acryloylation of enzymes. Acryloylated HRP and nanogel synthesis for comparison of the encapsulation efficiency with and without the introduction of the vinyl groups to the protein (**Figure 1**) was prepared according to our previous report.[6]

3.2 In situ polymerization/encapsulation. Commercial enzymes (3–60 μM, 2 mL in sodium phosphate 50 mM buffer, pH 6.1) were deoxygenated by bubbling N_2 through the solutions for 45 min. Sucrose (5%, w/v) was added to the enzyme solution, together with acrylamide (AAm) in deoxygenated sodium phosphate buffer (50 mM, pH 6.1) and *N*,*N*´-methylenebisacrylamide (MBAAm) in deoxygenated DMSO (10 % v/v, 33 mM). Unless otherwise mentioned, monomer ratios were kept constant (AAm/protein 6000:1 mol/mol; MBAAm/protein 1000:1 mol/mol). While bubbling nitrogen, ammonium persulfate (APS/protein 500:1 mol/mol) and tetramethylethylenediamine (TEMED/APS 2:1 w/w) were added to the enzyme/AAm/MBAAm mixture. In the case of HRP, 4-dimethylaminoantipyrine (AP, 1 mM final concentration) was additionally added as stabilizer for the heme prosthetic group. The reaction was kept under N_2 and shaken at room temperature for 2 h. SENs were dialyzed against PBS buffer to remove low-molar mass reagents and passed through a Sephadex G-75 column in order to remove non-encapsulated enzymes and protein-free polymer hydrogels.

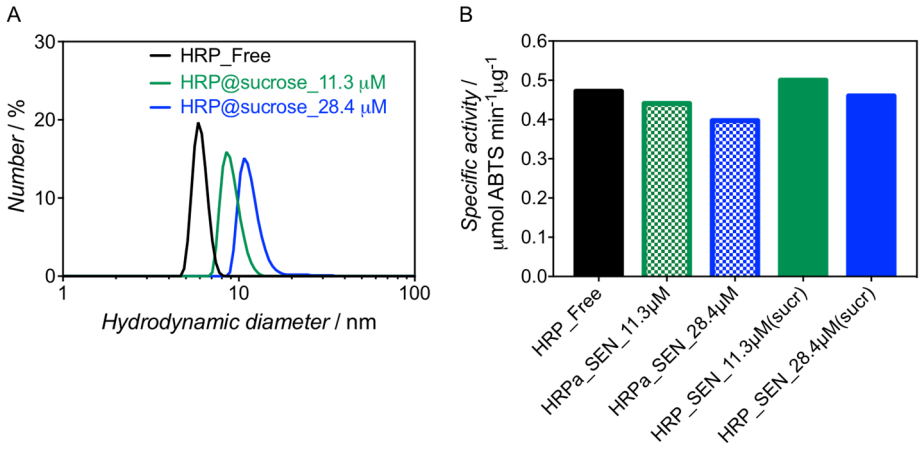

Figure S1. (A) Hydrodynamic diameter number distributions of SENs obtained by sucrose-doped encapsulation of HRP. B) Specific activity developed with ABTS of commercial HRP, SENs from acryloylated HRP, and SENs produced through sucrose-doped encapsulation. Activity was measured at 40 ºC using the parameters described above.

3.3 Evaluation of the effect of sucrose on the polymerization reaction

The effect of small carbohydrates on the nanogel thickness was examined by using the monosaccharides glucose, sorbitol, xylose, and fructose, and the disaccharides lactose, sucrose, and trehalose in the polymerization reaction (Figure 1C). The reaction in the absence of such additives was taken as a reference. Carbohydrates were used at 5 % w/v concentration in a typical encapsulation of BSA (10 μM, 50 mM sodium phosphate buffer, pH 6.1). The optimal sucrose concentration was screened at 0.1, 1.0, 5.0, and 10 % (w/v). After polymerization, unreacted reagents were removed by passing the solution through a Sephadex PD-10 column. Hydrodynamic diameters were measured by DLS to determine the gel thicknesses.

Furthermore, the effect of sucrose as an encapsulation enhancer was evaluated by incorporation of a chromophoric unit (by copolymerization with rhodamine 6G methacrylate, RMA) for a straightforward determination (Figure 1D). For quantification, a calibration curve was prepared beforehand: the UV-Vis spectra of four solutions of increasing RMA concentrations were

measured (1.17 µM, 2.94 µM, 5.88 µM and 29.42 µM; see Figure S2, left) and the maximum absorbance value was recorded. As RMA shows two overlapping maxima at 506 and 534 nm in PBS, the sum of their absorbances were used to plot the calibration curve (Figure S2, right), as well as for the calculations. A linear regression of these data yielded the equation $y = 0.086x$ ($r^2 = 0.999$).

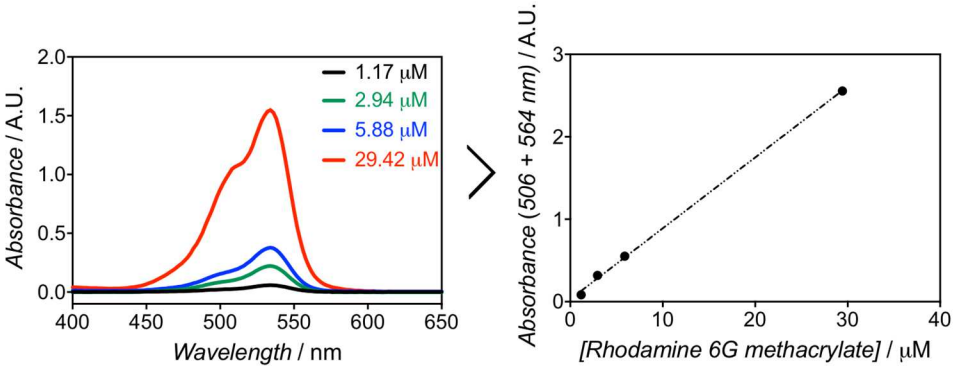

Figure S2. UV-Vis spectra of four solutions of RMA at various concentrations in PBS solution (left) and the corresponding linear calibration of characteristic absorbances *vs.* RMA concentration in PBS (right).

Three parallel experiments were carried out in order to determine the effect of sucrose as encapsulation enhancer. An aqueous solution of free HRP (22.7 µM, 2 mL) was first deoxygenated by bubbling N_2 for 45 min. Sample RMA_2% was prepared as follows: AAm (AAm/HRP 6000:1 mol/mol, 19.8 mg) in deoxygenated sodium phosphate buffer (50 mM, pH 6.1), and MBAAm (AAm/MBAAm 6:1 mol/mol, 7.5 mg) and RMA (AAm/RMA 50:1 mol/mol, 3.2 mg) in deoxygenated aqueous DMSO (15% v/v, 50 mM) were added to the HRP solution. and the resulting solution was kept under N_2 for 20 min. The crosslinking polymerization started upon addition of APS (APS/protein 500:1 mol/mol, 5.2 mg) and TEMED (TEMED/APS 1:1 mol/mol, 7.3 µL). The encapsulation was allowed to proceed for 2 h at room temperature. The

same procedure with specific modifications was used to prepare the rest of the samples, *i.e.*, RMA_2%@Sucrose_5% (HRP/AAm/MBAAm/RMA/APS/TEMED 1:6000:1000:120:500:500 in a 5% w/v sucrose solution) and RMA_10% (HRP/AAm/MBAAm/RMA/APS/TEMED 1:6000:1000:600:500:500). All samples were purified according to the same protocol. Encapsulated proteins were dialyzed against PBS to remove low-molar reagents and passed through a Sephadex G-75 column.

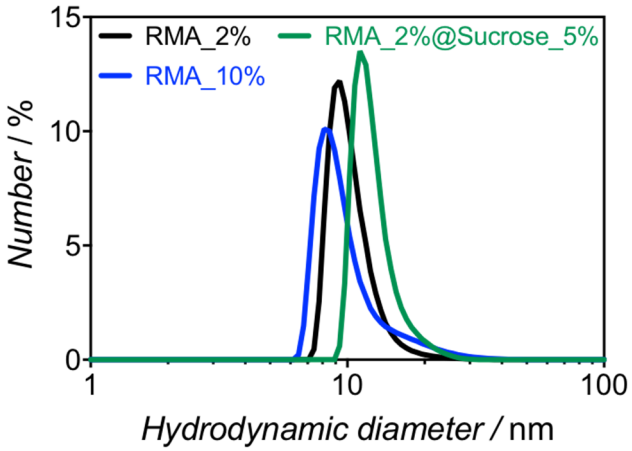

Figure S3. Hydrodynamic diameter number distributions of rhodamine-labeled HRP_SENs obtained by incorporation of RMA.

4. GOx as a case study

4.1 Tuning SEN shell thickness

Control over the polymeric shell thickness was achieved by varying the protein concentration in the encapsulation reaction, keeping all other component ratios constant (sucrose 5% (w/v; [protein]/[AAm] = 1:6000; [AAm]:[MBAAm] = 6:1; [AAm]:[APS] = 12:1). SENs were purified as aforementioned and the hydrodynamic diameter measured by DLS. Experiments were generally reproduced up to three times using the same protocol, yielding an average total error of 18 %. Results are summarized in **Table S1**.

Table S1. Number-average hydrodynamic diameter (D_n) values obtained by DLS for the synthesis of SENs with 5% w/v sucrose and corresponding calculated thicknesses for 9 different encapsulated proteins using a range of seeding protein concentrations (3.3 to 58.4 μM).

Sample	[Protein] (μM)	D_n (nm)	Thickness[a] (nm)	Sample	[Protein] (μM)	D_n (nm)	Thickness[a] (nm)
GOx_SEN1	3.3	8.0 ± 0.3	0.3 ± 0.0	CalB_SEN1	28.0	16.5 ± 1.3	3.3 ± 0.3
GOx_SEN2	6.7	8.6 ± 0.5	0.6 ± 0.0	CalB_SEN2	56.3	23.0 ± 2.2	6.5 ± 0.6
GOx_SEN3	10.0	10.3 ± 1.4	1.4 ± 0.2	HRP_SEN1	11.2	8.5 ± 0.1	1.4 ± 0.0
GOx_SEN4	13.4	10.3 ± 1.1	1.5 ± 0.2	HRP_SEN2	26.6	11.0 ± 0.6	2.6 ± 0.1
GOx_SEN5	16.7	11.5 ± 0.8	2.1 ± 0.1	HRP_SEN3	58.4	18.2 ± 1.1	6.2 ± 0.4
GOx_SEN6	20.1	11.8 ± 0.3	2.2 ± 0.1	β-Glu_SEN1	15.0	10.8 ± 2.4	1.6 ± 0.3
GOx_SEN7	23.5	12.5 ± 0.2	2.5 ± 0.1	β-Glu_SEN2	27.0	15.6 ± 3.5	4.0 ± 0.9
GOx_SEN8*	26.8	13.9	3.25	β-Glu_SEN3	38.0	17.7 ± 0.8	5.0 ± 0.2
GOx_SEN9	30.2	14.2 ± 0.4	3.4 ± 0.1	TvL_SEN1	17.0	10.2 ± 0.8	2.4 ± 0.2
GOx_SEN10	33.5	16.8 ± 1.0	4.7 ± 0.3	TvL_SEN2	28.0	13.7 ± 2.2	4.1 ± 0.7
GOx_SEN11**	26.8	9.0 ± 0.1	0.8 ± 0.0	CAT_SEN1*	13.0	7.7	1.3
PfE_SEN1	16.6	12.2 ± 0.5	1.9 ± 0.1	CAT_SEN2*	22.0	9.3	2.1
PfE_SEN2	25.0	13.7 ± 1.4	2.6 ± 0.3	CAT_SEN3*	31.0	13.5	4.2
PfE_SEN3	56.0	22.9 ± 5.0	7.3 ± 1.6	BSA_SEN1*	15.4	10.0	1.8
AOx_SEN*	26.0	12.8	3.2	BSA_SEN2*	30.1	12.0	2.8

[a]Thickness values were calculated by the subtraction of the contribution of the protein core itself (7.4 nm for GOx; 8.4 nm for PfE; 6.4 nm for AOx; 5.8 nm for HRP; 7.7 nm for β-Glu; 9.9 nm for CalB; 5.4 nm for TvL; 5.1 nm for CAT; and 6.4 nm for BSA) from the final diameter D_n measured by DLS and dividing the result by 2. *For these samples, a single run was carried out. **GOx_SEN11 was prepared using an increased amount of MBAAm crosslinker ([AA]/[MBAAm] = 2:1), as described further.

4.2 GOx_SEN chromatographic analysis. Samples GOx_SEN1 to GOx_SEN10 were dialyzed to remove low molecular mass compounds and sequentially eluted through a manually packed Sephadex G-75 column in phosphate buffer (50 mM, pH 6.5). Fractions of 0.5 mL were

collected and analyzed by UV-Vis spectroscopy. Chromatograms were then plotted at three distinct wavelengths: 230 nm (in red, indicating the presence of both polymer and protein), 280 nm (in green, shows the presence of protein and small contribution of the polymer), and 450 nm (purple, indicating only to the presence of GOx). These independent chromatograms are compiled in Figure S4.

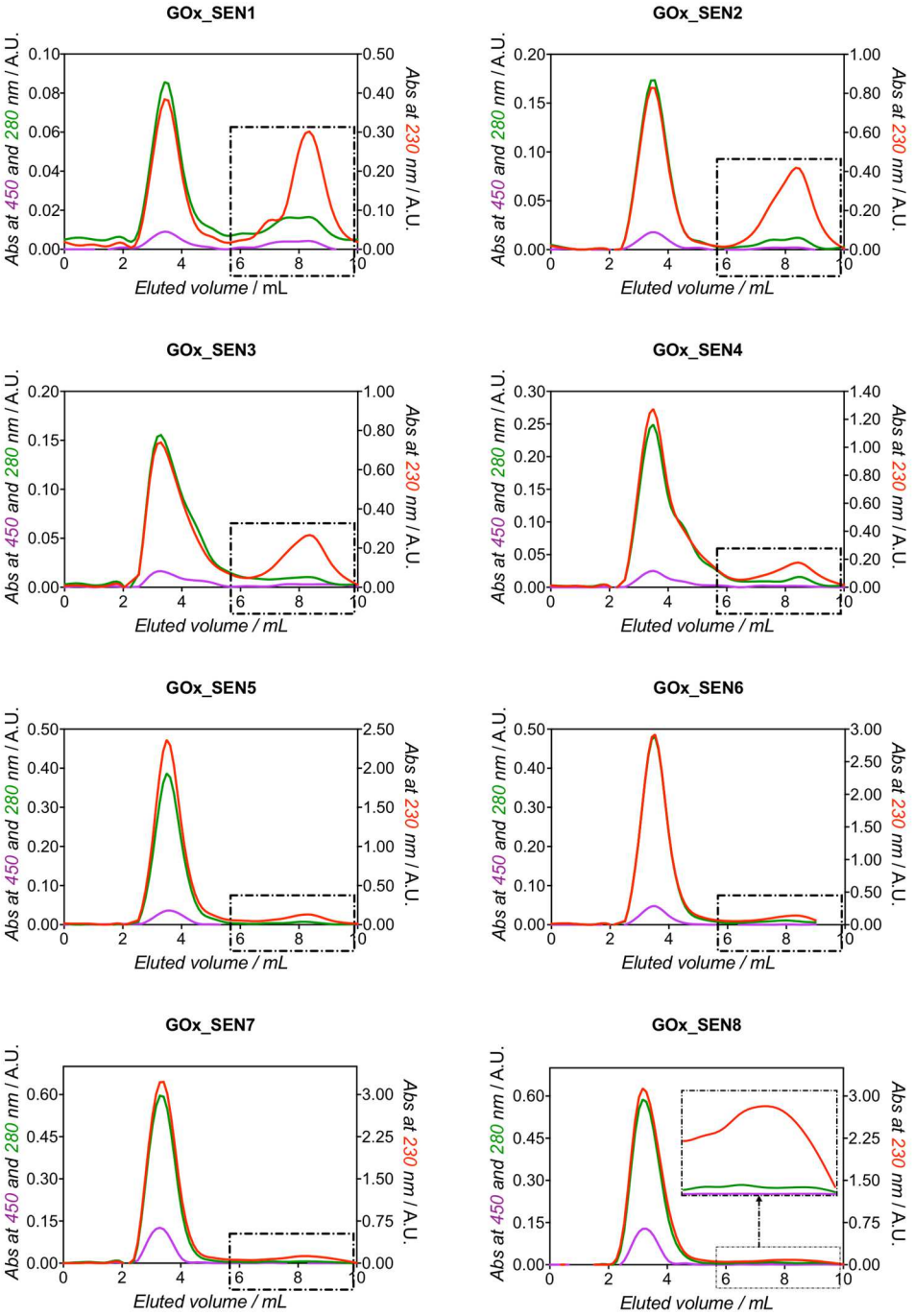

Figure S4. Size-exclusion chromatograms obtained by compiling data from the UV-Vis spectra of each eluted fraction of GOx_SEN1 to GOx_SEN10 samples at various absorbances: (left Y axes) 450 nm (purple traces) and 280 nm (green traces) and (right Y axes) 230 nm (red traces). The enlarged area on the elution volume range in GOx_SEN8 to GOx_SEN10 samples shows the presence of polymer species and, at the same time, an apparent absence of protein.

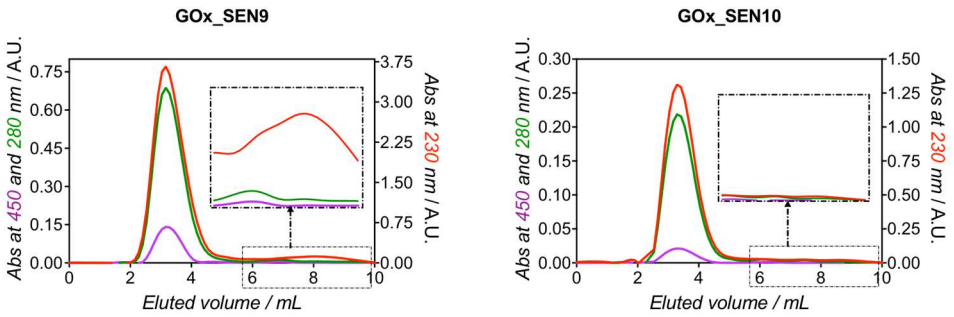

Figure S4 ***continued.***

Figure S5 shows in the same plot all the chromatograms obtained at 450 nm in order to evidence the encapsulation efficiency. Indeed, if present, non-encapsulated proteins appear in fractions eluting from 6.0 to 9.0 mL.

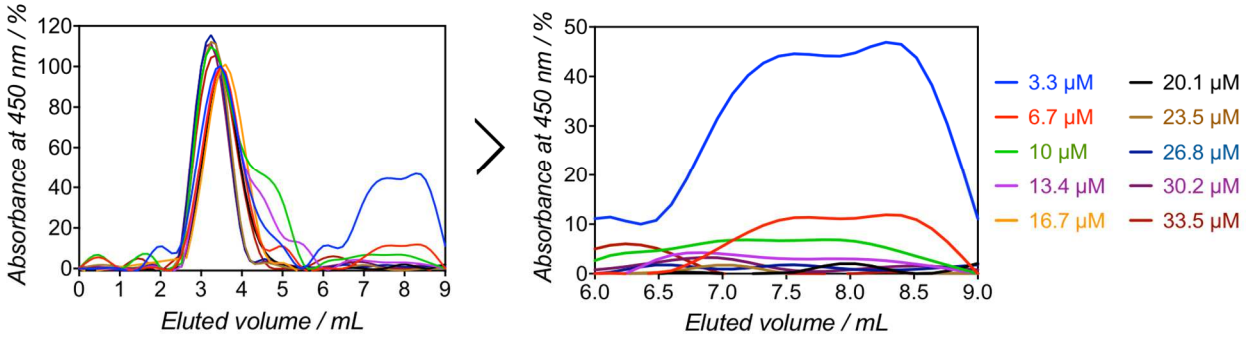

Figure S5. Size-exclusion chromatograms obtained at 450 nm for GOx_SEN1 to GOx_SEN10 samples. The region in which the non-encapsulated proteins are eluted is enlarged in order to depict the presence or absence of free protein for the different samples.

The amount of protein (in %) that was not encapsulated was determined by plotting the ratio of the average of absorbance at 450 nm in the free protein elution fractions (6.0–9.0 mL) compared to the total absorbance at 450 nm in both the free protein and the SENs elution region (2.5–4.0 and 6.0–9.0 mL). Encapsulations carried out without the addition of sucrose as additive clearly

led to higher amounts of non-encapsulated protein, as compared to experiments carried out with sucrose.

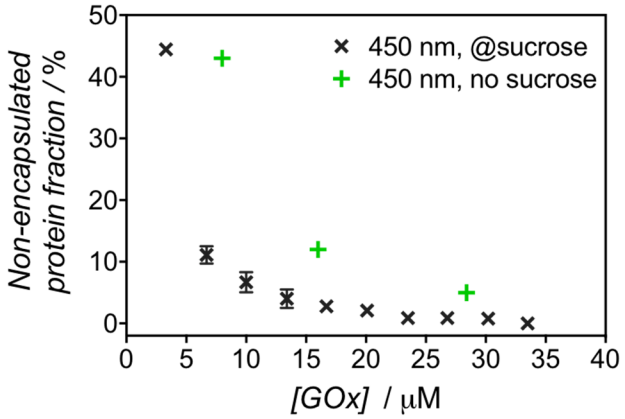

Figure S6. Fraction of non-encapsulated GOx as a function of initial protein concentration during SEN synthesis, as monitored by UV-Vis spectroscopy, with (black crosses) and without (green crosses) sucrose addition.

5. Extension of the methodology to other proteins

5.1 Thickness vs protein concentration dependence

SENs were prepared using the aforementioned sucrose-containing protocol and identical component ratios with a variety of enzymes: horseradish peroxidase (HRP), glucose oxidase (GOx), β-glucosidase (β-Glu), laccase (TvL), CalB lipase (CalB), alcohol oxidase (AOx), catalase (Cat), esterase (PfE), and bovine serum albumin (BSA). All SEN solutions were dialysed after synthesis and purified through a Sephadex G-75 column. **Table S1** summarizes the experiments, particularly the protein concentrations employed and the corresponding calculated thicknesses for each case according to the DLS data shown in **Figure S7**.

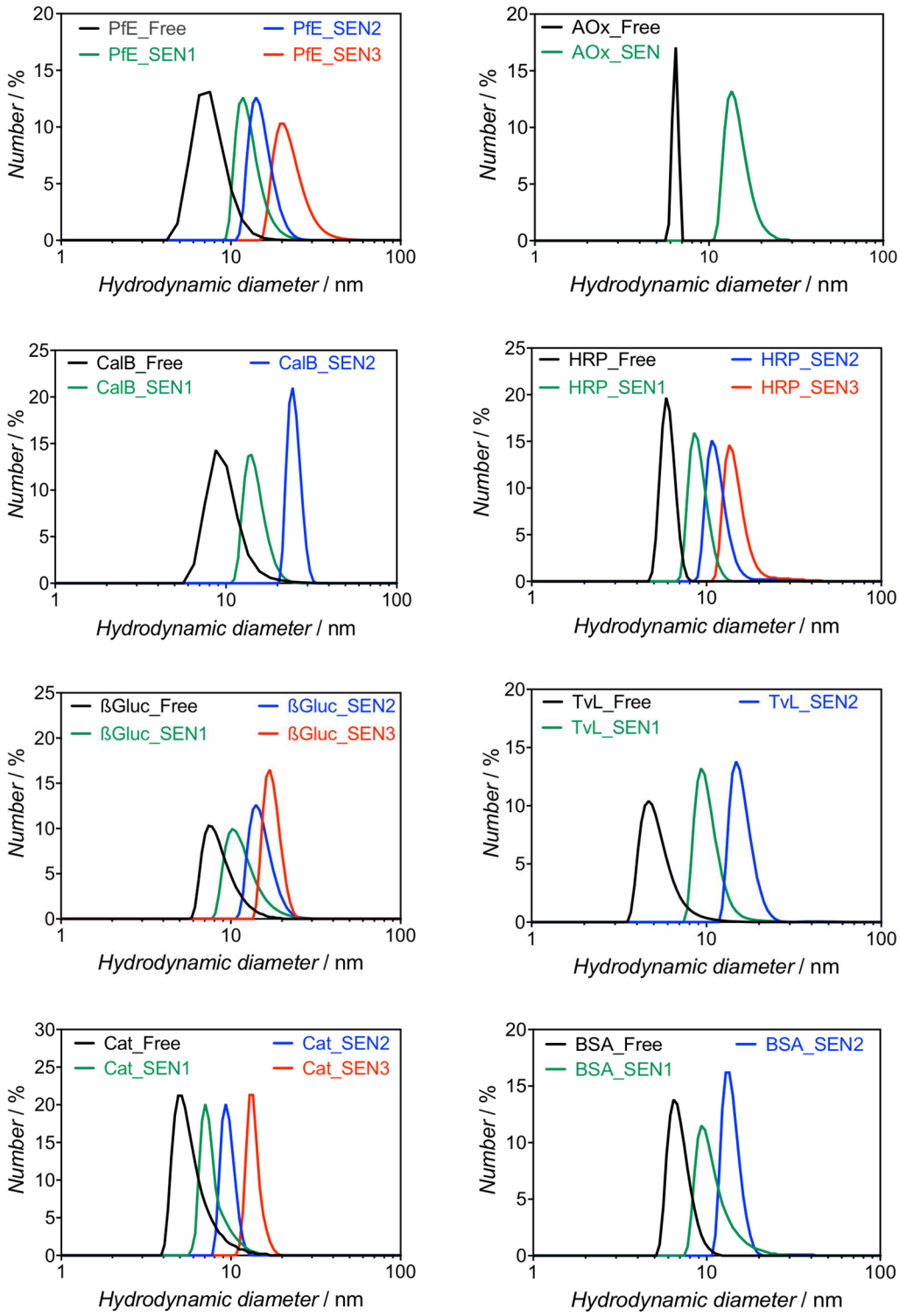

Figure S7. Number-average hydrodynamic diameter distributions for both free and encapsulated enzymes at various seeding protein concentrations.

5.2 Stabilization of laccase (TvL) at physiological conditions

Native TvL and its encapsulated counterparts, TvL_SEN1 and TvL_SEN2, at a concentration of 40 μM were assayed to oxidize ABTS (0.3 mM) in sodium phosphate buffer pH 7.0 and 37 ºC. While all of them showed a decreased activity compared to that at the optimal pH 4.0, encapsulated laccases showed higher oxidation rates than the commercial, non-encapsulated enzyme.

Table S2. Activity of laccase and laccase-based SENs (40 μM) at pH 7.0 and 37 ºC monitored by ABTS assay.

	Specific activity ($nM_{ABTS}\ min^{-1}\ mg_{protein}^{-1}$)
commercial TvL	1.25
TvL_SEN1	178
TvL_SEN2	186

6. Enzymatic activity tests

6.1 GOx

6.1.1. Determination of the kinetic parameters at different shell thicknesses

The k_{cat} values were determined for selected samples studied by chromatography: GOx_SEN2 (0.6 ± 0.0 nm thickness polyacrylamide shell), GOx_SEN5 (2.1 ± 0.1 nm), GOx_SEN7 (2.5 ± 0.1 nm) and GOx_SEN10 (4.7 ± 0.3 nm). As reference, the k_{cat} value for free GOx was also measured under the same conditions. Activity assays were performed in triplicate using 2% w/v solution of glucose in sodium phosphate buffer (30 mM, pH 6.0), ABTS (0.27 mM), HRP (0.01 mg mL^{-1}) at 40°C. The oxidized ABTS production was monitored through the increase of absorbance at 416 nm. Protein concentrations ranging from 0 to 8 nM were employed and the measured initial velocities (in $M_{glucose}$ min^{-1}) were plotted against the protein concentration used for the reaction. k_{cat} values were obtained from the slopes of these graphs.

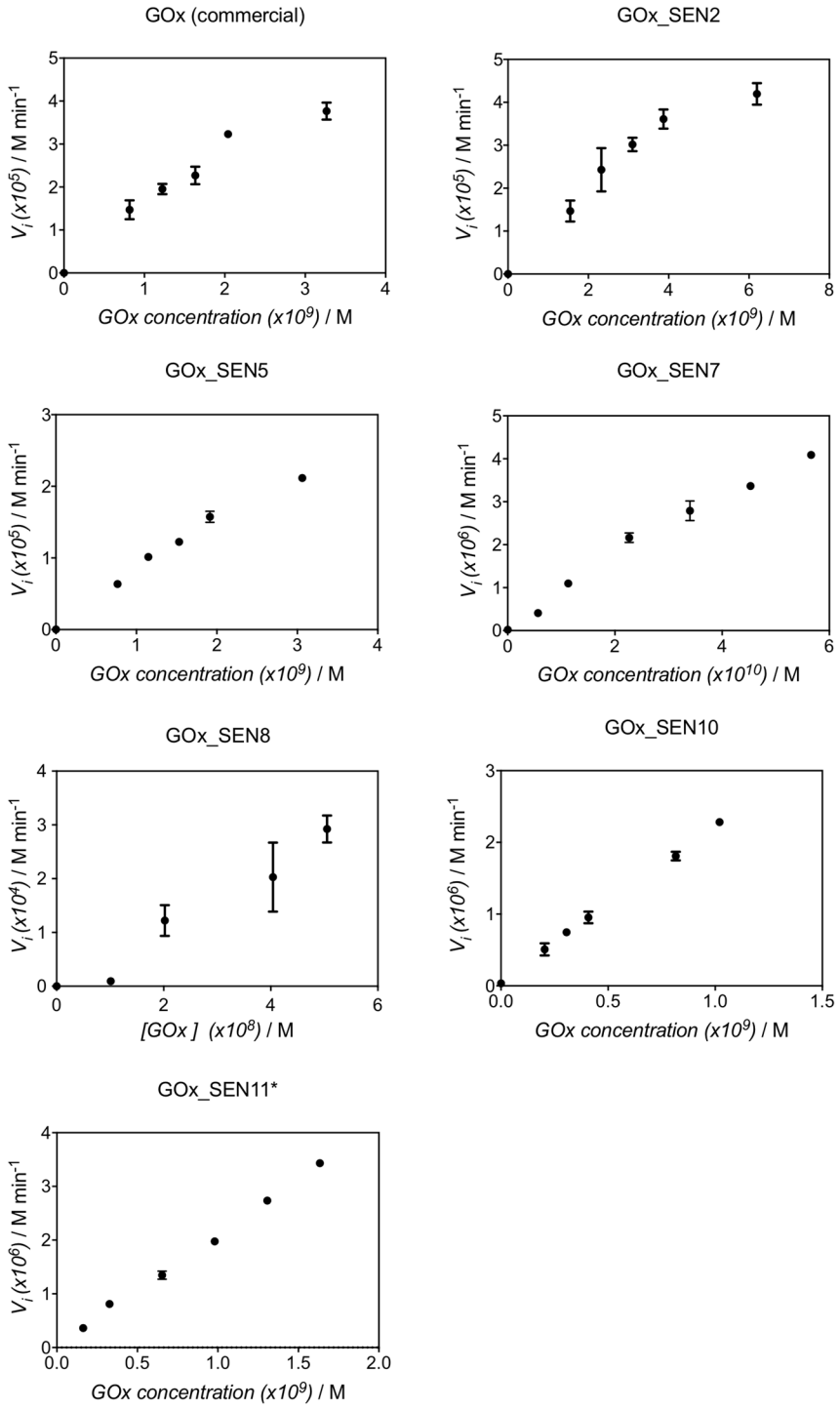

Figure S8. Obtained kinetic plots for commercial GOx, GOx_SEN2, GOx_SEN5, GOx_SEN7, GOx_SEN10, and GOx_SEN11 samples that were used for the calculation of k_{cat} values. *GOx_SEN11 was prepared using a decreased monomer concentration and an increased crosslinker ratio ([AAm]/[MBAAm] = 2:1). A detailed description is provided further.

Table S3. k_{cat} values measured for commercial GOx and its encapsulated counterparts under same conditions (2% (w/v) glucose, 0.27 mM of ABTS, 0.01 mg mL^{-1} of HRP in phosphate buffer at pH 6.0 and 40 ºC).

	k_{cat} (s^{-1})	k_{cat}(GOx_SEN)/k_{cat}(GOx)	*Shell thickness average (nm)*
GOx (commercial)	162.9 ± 20.0	-	-
GOx_SEN2	158.1 ± 7.1	0.97	0.6 ± 0.0
GOx_SEN5	135.8 ± 4.8	0.83	2.1 ± 0.1
GOx_SEN7	120.0 ± 7.2	0.74	2.5 ± 0.1
GOx_SEN8*	98.1 ± 10.9	0.60	3.3
GOx_SEN10	36.2 ± 0.4	0.22	4.7 ± 0.
GOx_SEN11	32.2 ± 3.8	0.20	0.8 ± 0.0

*Shell thickness measurement for GOx_SEN8 was performed once.

6.1.2. Stability of GOx_SENs

pH stability. The stability of the GOx_SEN samples over a range of pH spanning values from 3.0 to 9.4 was tested. For this purpose, different buffers (100 mM) were used: sodium citrate pH 3.01 and pH 4.04; sodium acetate pH 4.98 and 6.03; sodium phosphate pH 7.05 and pH 8.10; and sodium bicarbonate pH 9.40. GOx_SENs were incubated 5 min at 40 °C in these buffers containing 2 % (w/v) of glucose at a protein concentration of 10 nM. From these solutions, an aliquot of 2 to 8 µL was added to a 200 µL of ABTS (2.7 mM) and HRP (1 mg mL^{-1}) in sodium citrate buffer (100 mM, pH 4.5) mixture, and the ABTS oxidation was monitored at 416 nm for 5 min.

Thermostability, effect of trypsin, and stability upon storage of GOx nanogels. Thermostability of GOx nanogels were tested using the GOx_SEN5 hybrid (2 uM aliquots in sodium phosphate

30 mM, pH 6.1). Each solution was heated to 65 °C and aliquots were taken after 5, 15, 25, and 40 min of incubation and cooled down on ice before the measurement of their activity (see Figure S9A).

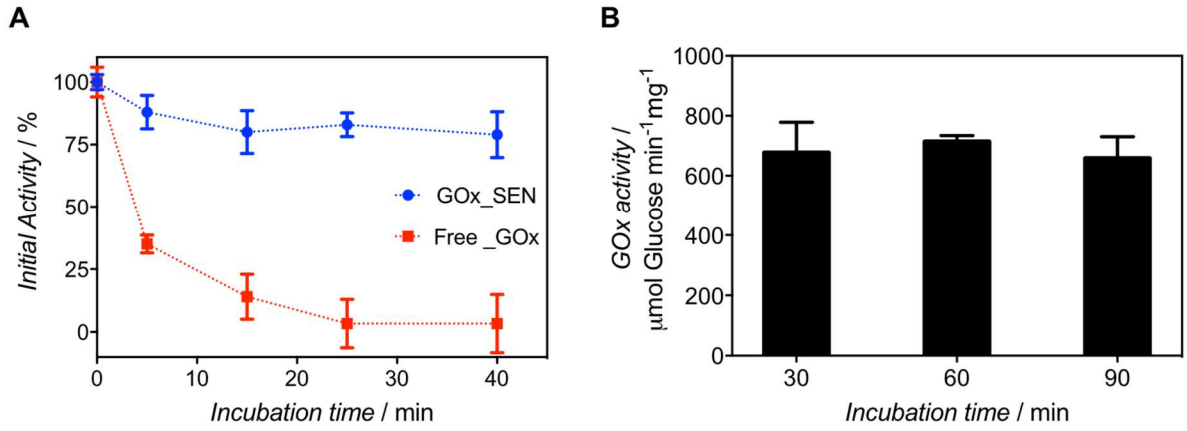

Figure S9. A) Relative activity (%) of free GOx and GOx_SEN5 as a function of incubation time at 65 °C. B) GOx_SEN7 activity upon exposure to trypsin for different times.

A GOx_SEN7 solution (15 µM in sodium phosphate 30 mM, pH 6.1) was mixed with trypsin (1 µM) at 37 °C and GOx activity was measured after 30, 60 and 90 min (see Figure S9B). In addition, GOx nanogels were kept at room temperature while this study was performed, showing no precipitation or significant change in their initial activity. Besides, no activity loss was observed upon freeze-dry-redissolve or freeze-thaw treatments.

6.1.3. Production of GOx_SEN with invariable activity over the entire pH range *(GOx_SEN11)*

The GOx_SEN11 sample was prepared using different encapsulation conditions. Free GOx (26.8 µM, 2 mL) in sodium phosphate buffer (50 mM, pH 6.1) was deoxygenated by bubbling N_2 for 45 min. Sucrose (5%, w/v), AAm (GOx/AAm 1:1000, 53.3 µmol, 3.79 mg) in deoxygenated sodium phosphate buffer (50 mM, pH 6.1), and MBAAm (AAm/MBAAm 2:1 mol/mol, 26.6

μmol, 4.1 mg) in deoxygenated DMSO (15% v/v, 50 mM) were added to deoxygenated protein and kept under N_2 bubbling for 20 min. Upon addition of APS (APS/protein 500:1 mol/mol, 6.0 mg) and TEMED (TEMED/APS 1:1 mol/mol, 8.5 μL), the polymerization was allowed to proceed for 2 h at room temperature. Encapsulated GOx were purified by dialysis and column chromatography using a hand-packed Sephadex G-75 column.

6.2. Other enzymes

k_{cat} values were determined for some of the SENs in order to reveal the adverse effect of the polyacrylamide layer thickness on the substrate diffusion under normal conditions. Activity measurements were performed at 40 °C in triplicate, with an enzyme concentration ranging from 0 to 0.8 μM and fixed substrate concentration of 1 mM of *p*-nitrophenyl-ß-glucopyranoside (pNPGluc) for ß-Glucosidase, 0.8 mM of *p*-nitrophenylbutyrate ($pNPC_4$) for PfE esterase and CalB lipase, and 0.3 mM of ABTS for TvL laccase. Initial velocities were measured for each enzyme concentration and plotted as M^{-1} min^{-1} of catalyzed substrate. k_{cat} values were calculated from the slopes of the linear fits and listed in Table S3.

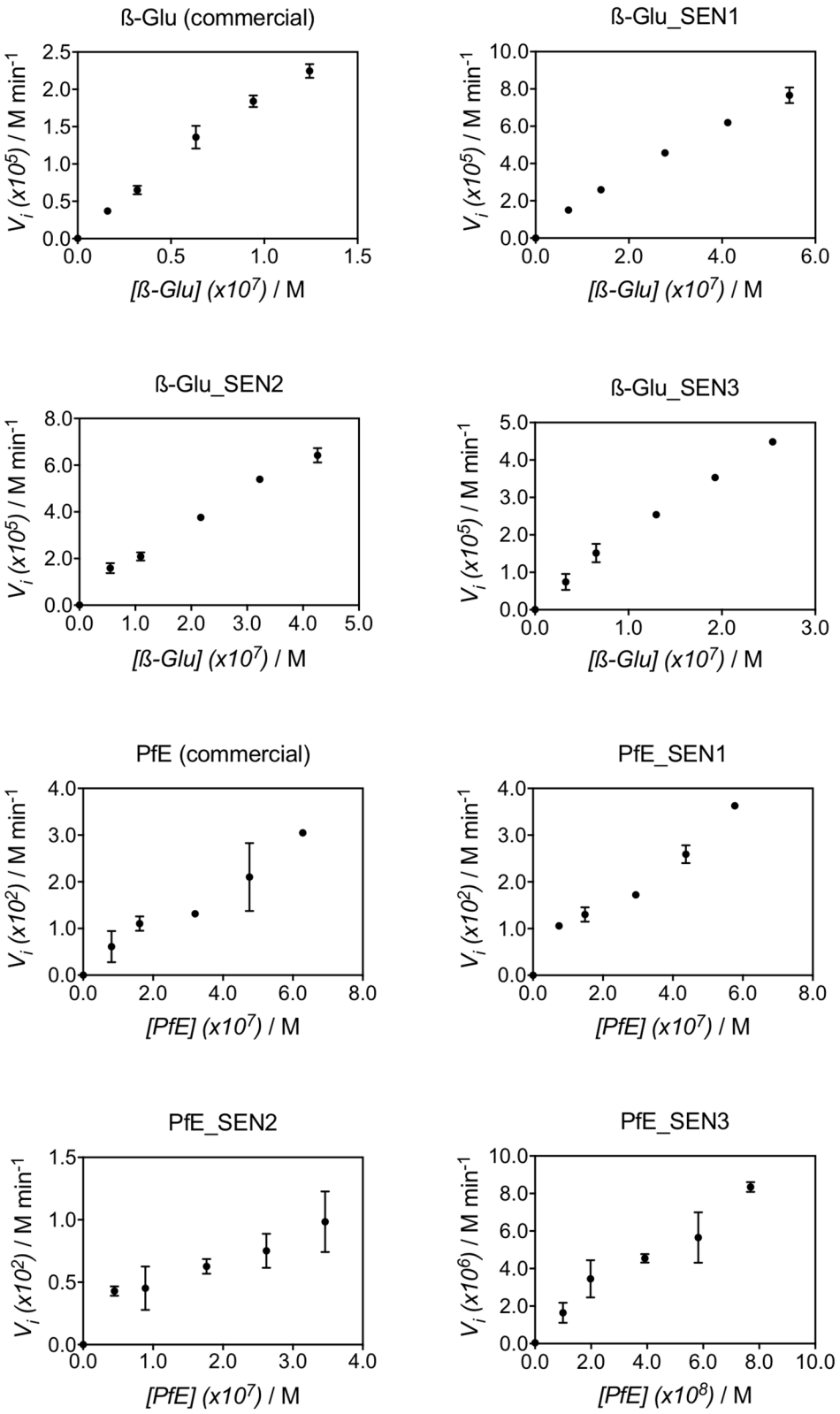

Figure S10. Kinetic plots used for k_{cat} calculation.

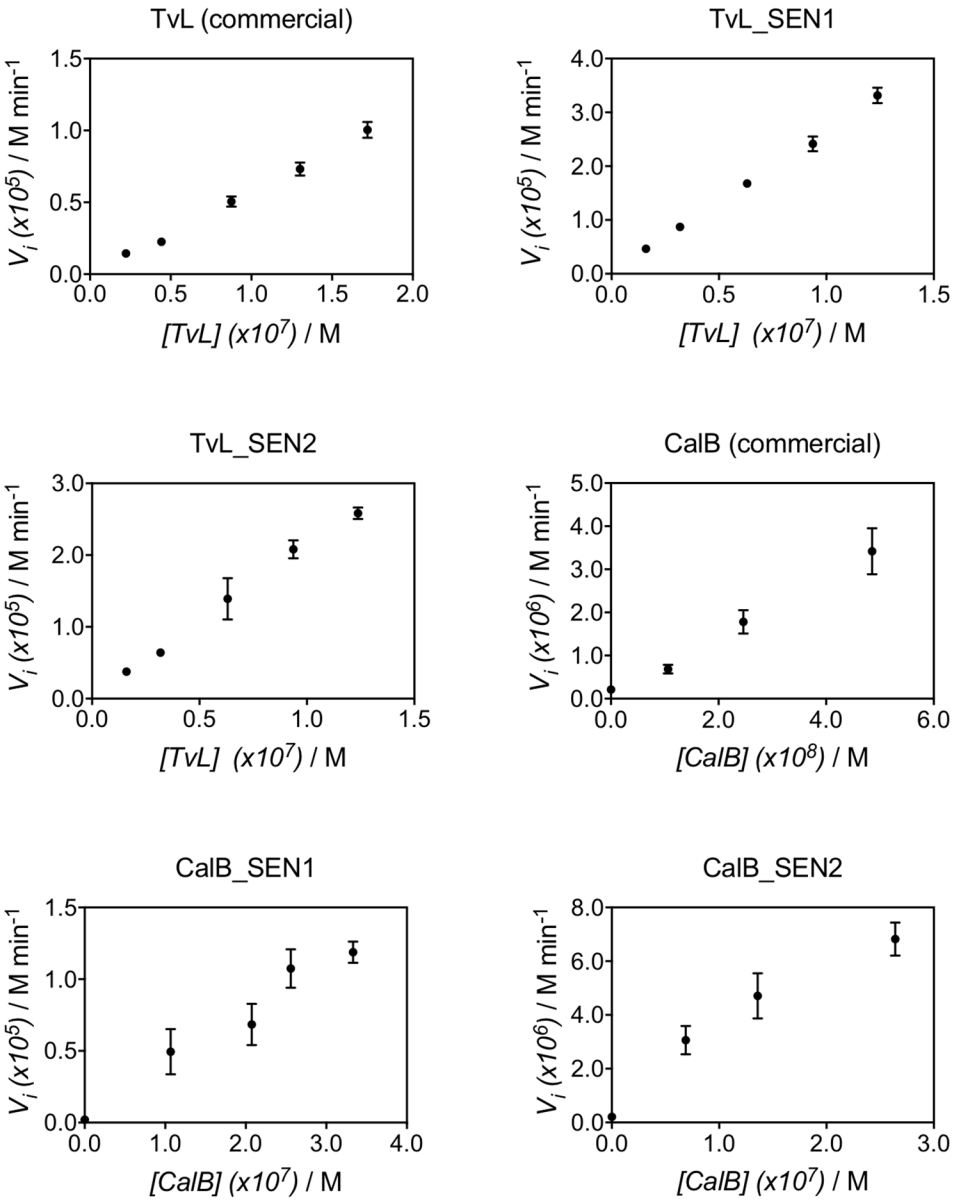

Figure S10 ***continued.***

Table S4. k_{cat} values of commercial and encapsulated enzymes measured under the same conditions.

	k_{cat} (min^{-1})	k_{cat}(SEN) /k_{cat}(commercial)	*Shell thickness (nm)*
β-Glu (commercial)	182.8 ± 8.5	1	-
β-Glu_SEN1	173.0 ± 6.9	0.95	1.6
β-Glu_SEN2	149.9 ± 9.1	0.82	4.0
β-Glu_SEN3	108.1 ± 6.9	0.59	5.0
PfE (commercial)	39881 ± 4028	1	-
PfE_SEN1	50250 ± 5665	1.26	1.9
PfE_SEN2	27120 ± 4108	0.68	2.6
PfE_SEN3	8773 ± 962	0.22	7.3
TvL (commercial)	257.8 ± 1.3	1	-
TvL_SEN1	263.0 ± 4.1	1.02	2.4
TvL_SEN2	212.5 ± 5.6	0.82	4.1
CalB (commercial)	51.7 ± 4.4	1	-
CalB_SEN1	40.3 ± 6.3	0.78	3.3
CalB_SEN2	24.1 ± 4.0	0.47	6.6

7. Single-Particle Analysis

7.1. Blank experiment

AAm and MBAAm were subjected to polymerization in the absence of protein while keeping the concentrations similar to those upon SEN synthesis. AAm (9.6 mg, 135 µmol), MBAAm (3.5 mg, 22.7 µmol), and sucrose (5% w/v) were dissolved in sodium phosphate buffer (50 mM, pH 6.1) – DMSO (10% v/v) mixture. This mixture was deoxygenated by bubbling N_2 for 45 min. While bubbling nitrogen, APS (2.6 mg, 11.4 µmol) and TEMED (1.72 µL, 11.4 µmol) were thoroughly added to the solution and the polymerization was kept under nitrogen and shaken at

room temperature for 2 h. The polyacrylamide particles were dialyzed against PBS to remove low-molar mass reagents. The corresponding DLS data is shown in Figure S11.

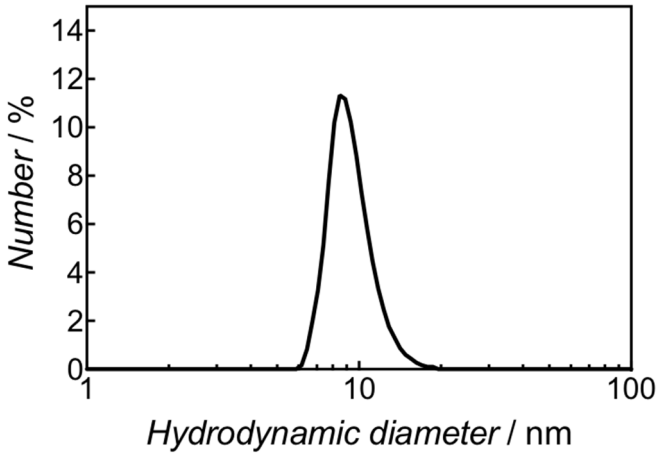

Figure S11. Hydrodynamic diameter number distribution obtained for polyacrylamide particles obtained in the blank experiment.

7.2. Calibration curves

In order to allow for further calculations and to determine the amount of fluorophores incorporated in the SENs, UV-Vis calibration curves for Alexa Fluor 647 and rhodamine-PEG-SH were established in PBS buffer (Figure S12).

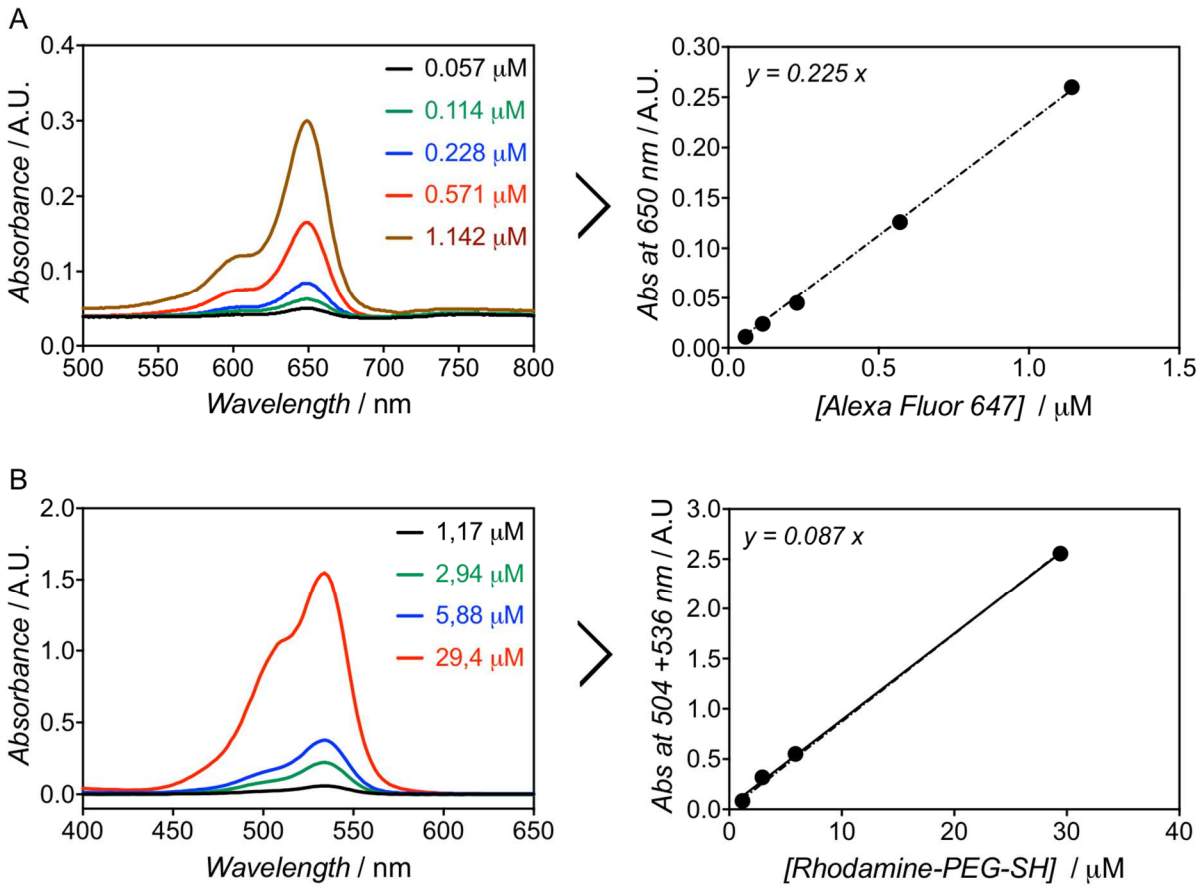

Figure S12. UV-Vis spectra and calibration curves for Alexa Fluor 647 (A) and rhodamine-PEG-SH (B) in PBS.

7.3. Catalyst selection for thio-Michael addition-based hydrogel labeling.

In order to selectively label the polymeric shell, we targeted the residual double bonds in the crosslinked network by thio-Michael addition with rhodamine-PEG-thiol (Rho-PEG-SH). This thiol-ene reaction was first optimized using two different catalysts, DIPEA and TCEP. The catalyst concentrations remained constant (1 mM), while the Rho-PEG-SH:SEN molar ratio was set to 10, 20, and 30. The SENs molar concentration was assumed identical to the protein concentration. After the reaction, non-reacted Rho-PEG-SH was removed using centrifugal filtration with 10 kDa membrane filters. The amount of grafted Rho_PEG-SH was then

determined by measuring a UV-Vis spectrum and using the previously established calibration curve (Figure S12B).

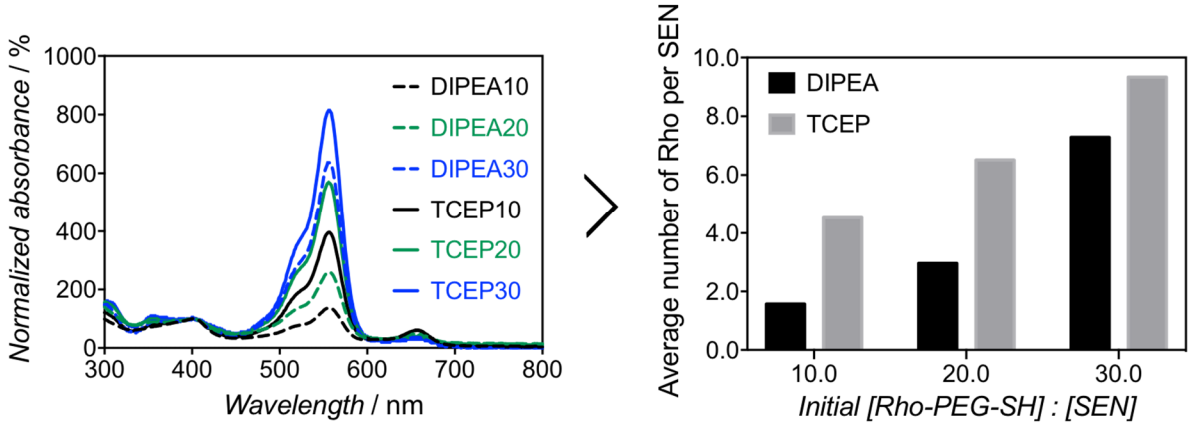

Figure S13. UV-Vis spectra of rhodamine-labeled SENs after the reaction with various molar ratios of Rho_PEG-SH:SEN in the presence of DIPEA or TCEP. The number next to the catalyst name corresponds to the initial [Rho-PEG-SH]:[SEN] molar ratio; B) Average number of rhodamine molecules grafted per SEN as a function of the initial [Rho-PEG-SH]:[SEN] molar ratio.

The evaluation of the maximum number of rhodamine molecules which can be grafted per nanogel was performed using TCEP (1 mM in 20 mM Tris-HCl buffer pH 7.1) and extending the initial [Rho-PEG-SH]:[SEN] ratio to 200. Results were nicely fitted to a saturation curve (r^2 = 0.992) and gave a maximum average number of rhodamine of 18.8 per SEN.

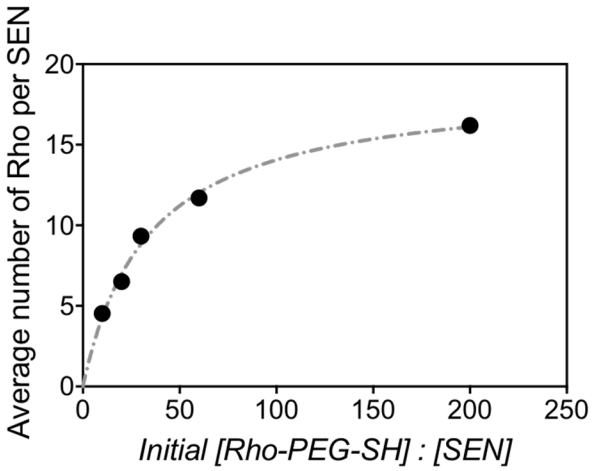

Figure S14. Average number (Av.No.) of rhodamine molecules grafted per SEN as a function of the initial Rho-PEG-SH:SEN molar ratio (In.Rat.). Values were fitted to a saturation curve (Av.No. = (18.84 * [In.Rat.]) / (34.03 + [[In.Rat.]).

7.4. Labeling of HRP

HRP was labeled with Alexa Fluor 647 by amidation at lysine side chains. For this, the activated NHS ester of the carboxylic acid derivative of Alexa Fluor® 647 was synthesized in situ. Alexa Fluor 647-COOH (2.5 mg, 0.002 mmol) was premixed with EDC-HCl (3 equivalents) and NHS-OH (3 equivalents) in 500 µL of dry DMF for 2 h at 25 °C. A solution of HRP (1 mL, 2.5 mg mL^{-1}) in freshly prepared sodium phosphate buffer (200 mM, pH 8.3) was reacted with the premixed solution of Alexa Fluor 647-NHS for 1.5 h at 37 °C and overnight at 4 °C. Excess, unreacted fluorophore was removed by dialysis (10 kDa membrane, 10 buffer exchange cycles) and the buffer was exchanged to 20 mM sodium phosphate, pH 6.0. This sample was kept in the dark (also for the next steps). According to the UV-Vis spectrum of the final product HRP@647 (Figure S15) and the pre-established calibration curve (Figure S12A), an average of 2.2 Alexa Fluor molecules per HRP protein were grafted.

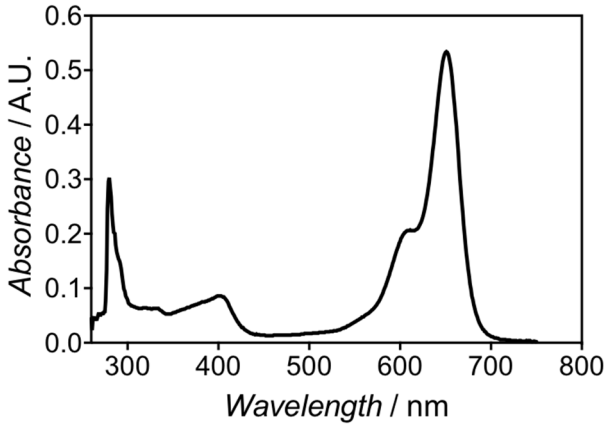

Figure S15. UV-Vis spectrum of HRP@647 obtained by labeling of HRP with Alexa Fluor 647.

7.5. Encapsulation of labeled HRP

HRP@647 (0.5 mg mL^{-1}, 1 mL) was used for the encapsulation, using the same conditions as described before ([HRP]/[AAm]/[MBAAm]/[APS] = 1:6000:1000:500, 5% (w/v) sucrose). These core-labeled nanogels were purified by dialysis and further characterized by UV-Vis spectroscopy and DLS (Figure S16). A number-average hydrodynamic diameter of 8.7 nm was determined.

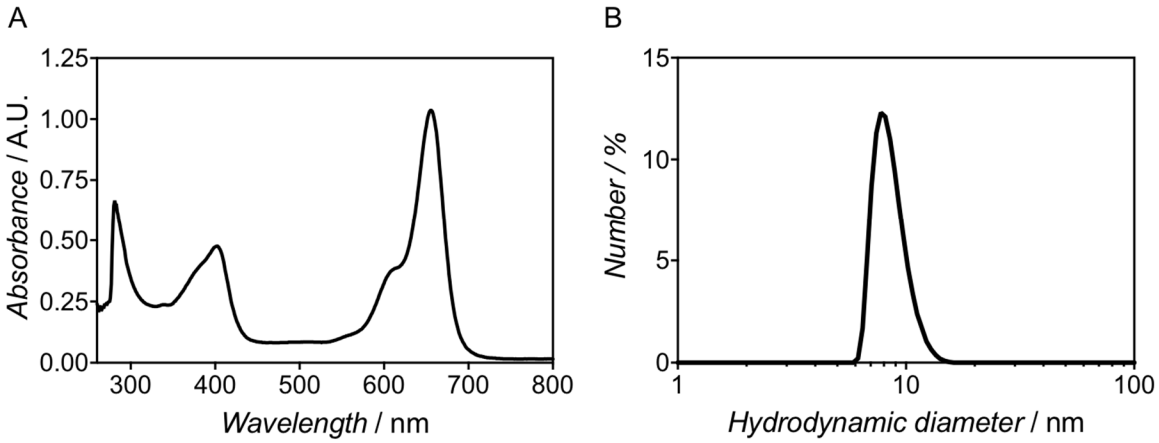

Figure S16. (A) UV-Vis spectrum of HRP@647_SEN. (B) Hydrodynamic diameter number distribution obtained for HRP@647_SEN.

7.6. Labeling of the shell of core-labeled SENs

Following the preliminary study on the labeling of SENs by thio-Michael addition (Figures S13 and S14), we designed a reaction targeting 2 to 5 rhodamine molecules per SEN. For single-particle high-resolution microscopy experiments, it is important to keep the number of fluorophores in low ratio concentrations. Having this in mind, we employed a SEN/Rho-PEG-SH molar ratio of 1:5. HRP@647_SEN (20 µL, 2.72 nmol) was mixed with Rho-PEG-SH (10 µL, 13.6 nmol) and TCEP (10 µL, 1 mM). The final reaction volume was set to 100 µL using phosphate buffer (30 mM, pH 6.0). The reaction mixture was kept for 1 h at 37 °C. Non-grafted Rho-PEG-SH was sequentially removed, first by dialysis (10 kDa MWCO membrane) and then by centrifugation using spin filters of 30 kDa MWCO, washing the sample with phosphate buffer (30 mM, pH 6.0) and Tween 20 (0.01% v/v) in order to remove adsorbed material.

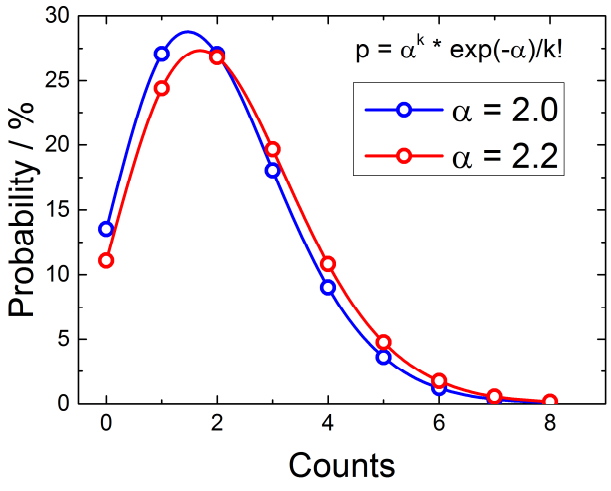

Figure S17. Poisson distributions illustrating the fractional populations of species with different numbers of labels, assuming average labeling ratios of 2.0 (blue) or 2.2 (red), respectively.

7.7. Single-particle burst coincidence analysis

Fluorescence time traces (Figure S18) were analyzed by employing in-house developed software using Matlab (MathWorks, Natick, MA, USA). Based on their arrival times within each 100 µs two-color alternating excitation cycle, photons were assigned to green and red excitation phases and binned to obtain photon numbers corresponding to green and red burst intensities, I_{GG} and I_{GR}, under 532 nm (green) excitation, and I_{RG} (≈ 0) and I_{RR} under 637 nm (red) excitation, respectively. All intensities were corrected for background and spectral cross-talk. For subsequent fluorescence coincidence analysis (FCA) of photon bursts from individual particles diffusing through the confocal volume, only bursts with total intensity $I_{GG} + I_{GR} + I_{RR}$ above 20 counts were used in the analysis to reject spurious events (noise). The apparent FRET efficiency values of individual bursts were calculated from the intensities I_{GG} and I_{GR} as $E = I_{GR}/(I_{GR} + I_{GG})$.

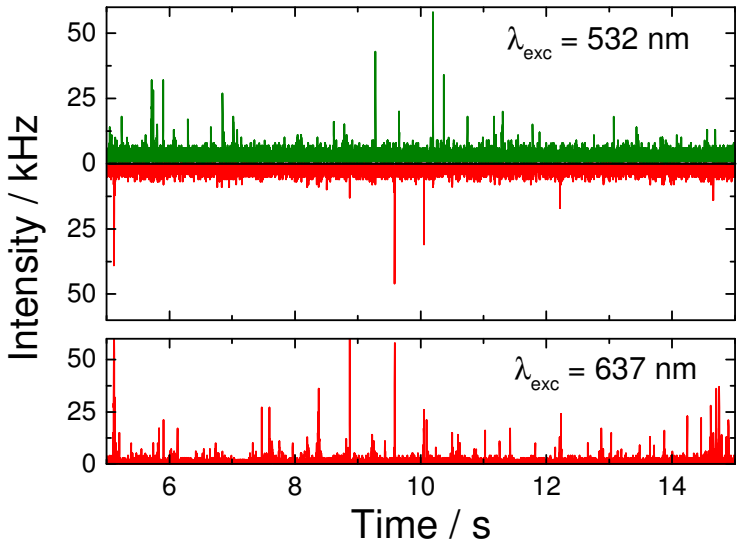

Figure S18. Fluorescence time-trace of freely diffusing particles obtained by using alternating 532 nm (green) and 637 nm (red) excitation. The upper panel shows the fluorescence intensity in the green and the red detection channels under green excitation (red due to FRET). In the lower panel, the corresponding fluorescence signal in the red detection channel under red excitation is shown.

8. References

(1) Madsen, J.; Warren, N. J.; Armes, S. P.; Lewis, A. L. Synthesis of Rhodamine 6G-Based Compounds for the ATRP Synthesis of Fluorescently Labeled Biocompatible Polymers. *Biomacromolecules* **2011**, *12*, 2225–2234.

(2) Bradford, M. M. A Rapid and Sensitive Method for the Quantitation of Microgram Quantities of Protein Utilizing the Principle of Protein-Dye Binding. *Anal. Biochem.* **1976**, *72*, 248–254.

(3) Heyes, C. D.; Kobitski, A. Y.; Amirgoulova, E. V.; Nienhaus, G. U. Biocompatible Surfaces for Specific Tethering of Individual Protein Molecules. *J. Phys. Chem. B* **2004**, *108*, 13387–13394.

(4) Kobitski, A. Y.; Nierth, A.; Helm, M.; Jäschke, A.; Nienhaus, G. U. Mg^{2+}-Dependent Folding of a Diels-Alderase Ribozyme Probed by Single-Molecule FRET Analysis. *Nucleic Acids Res.* **2007**, *35*, 2047–2059.

(5) Dammertz, K.; Hengesbach, M.; Helm, M.; Nienhaus, G. U.; Kobitski, A. Y. Single-Molecule FRET Studies of Counterion Effects on the Free Energy Landscape of Human Mitochondrial Lysine tRNA. *Biochemistry* **2011**, *50*, 3107–3115.

(6) Beloqui, A.; Baur, S.; Trouillet, V.; Welle, A.; Madsen, J.; Bastmeyer, M.; Delaittre, G. Single-Molecule Encapsulation: A Straightforward Route to Highly Stable and Printable Enzymes. *Small* **2016**, *12*, 1716–1722.